



HAL
open science

Experimental investigations of the critical values of J-integral and crack tip opening displacement (CTOD) of high-density poly-ethylene PE100 elbow

Manel Dallali, Z. Azari, C. Schmitt, Julien Capelle, E. Hadj-Taïeb

► To cite this version:

Manel Dallali, Z. Azari, C. Schmitt, Julien Capelle, E. Hadj-Taïeb. Experimental investigations of the critical values of J-integral and crack tip opening displacement (CTOD) of high-density poly-ethylene PE100 elbow. *Engineering Failure Analysis*, 2022, 131, pp.105834. 10.1016/j.engfailanal.2021.105834 . hal-04145380

HAL Id: hal-04145380

<https://hal.univ-lorraine.fr/hal-04145380v1>

Submitted on 22 Jul 2024

HAL is a multi-disciplinary open access archive for the deposit and dissemination of scientific research documents, whether they are published or not. The documents may come from teaching and research institutions in France or abroad, or from public or private research centers.

L'archive ouverte pluridisciplinaire **HAL**, est destinée au dépôt et à la diffusion de documents scientifiques de niveau recherche, publiés ou non, émanant des établissements d'enseignement et de recherche français ou étrangers, des laboratoires publics ou privés.



Distributed under a Creative Commons Attribution - NonCommercial 4.0 International License

Experimental investigations of the critical values of J-integral and crack tip opening displacement (CTOD) of high-density poly-ethylene PE100 elbow

M. Dallali^{a,b}, Z. Azari^b, C. Schmitt^b, J. Capelle^b, E. Hadj-Taïeb^a

^a Laboratoire de Mécanique des Fluides Appliqués, Génie des Procédés et Environnement, Ecole Nationale d'Ingénieurs de Sfax, BP 1173, 3038, Sfax, Tunisie

^b Laboratoire d'étude des Microstructures et de mécanique des matériaux (LEM3), Ecole Nationale d'Ingénieurs de Metz, Université de Lorraine, 57000 Metz, France

ABSTRACT

The present study aims to characterize the cracking behaviour of high-density poly-ethylene (HDPE) pipe elbow. Experimental studies were performed to determine the mechanical behaviour of HDPE and study the anisotropy of the material. Tension tests were performed on compact tension (CT) specimens to identify the toughness value, expressed by the critical value of the J-integral J_{Ic} . These tests were carried out on specimens cut from a PE100 plate with a different orientation angle with respect to the extrusion direction. The testing results have shown that HDPE can be considered as an isotropic material. The methods used to calculate the J_{Ic} value resulted in different values. Due to these uncertainties, a study of a failure criteria using crack tip opening displacement (CTOD) was proposed and conducted. The combination of the J-integral and "CTOD" method gave the possibility to determine for the critical value of the J-integral as a value of the fracture toughness of the HDPE. The obtained results suggest that the value of 8.4 kJ/m² can be considered as the J_{Ic} fracture toughness required to initiate the crack for the HDPE.

Keywords: HDPE elbow, J-integral, J-R curve, CTOD, J_{Ic}

Nomenclatures

a	defect depth
a ₀	Original crack length
c ₁	Constant
c ₂	Constant
CT	Compact Tension
CTOD	Crack Tip Opening Displacement
CTOA	Crack Tip Opening Angle

E	Young's modulus
HDPE	High-density polyethylene
K	Stress Intensity Factor
u	Displacement
J	J-integral
J _{1c}	J-integral critical value
SZW	Stretched Zone Width
U	Energy
U _i	Indentation energy
U _T	Total energy
α	Orientation angle
$\dot{\epsilon}$	Strain rate
σ_y	Yield stress
σ_u	Ultimate strength
η	Geometric factor
Δa	Crack extension

1. Introduction

Water scarcity is considered among the most dangerous problems facing humanity. A study conducted in 2015 has stated that water scarcity will be threatening more than 40% of the world population by 2050 [1]. Therefore, ensuring a sustainable management of this resource has never been more vital.

One of the aspects of sustaining this life-depending resource is the minimization of leaks. Indeed, leakages in drinking-water supply networks can cause the loss of a huge amounts of water. Moreover, drinking water resources are subjected to contamination in the presence of leaks. A leakage in water distribution networks (WDN) is mainly caused by a pipe rupture. It is considered a frequent phenomenon in urban zones and in general it is started with a defect. Engineers and researchers depend on the science of fracture mechanics to study the structural integrity of pipelines. However, the behaviour of pipelines presenting a defect is quite different from one material to another. For instance, steel pipes are treated differently from plastic pipes since the latter present a completely different mechanical behaviour.

It is worth noting that in the last 40 years, plastic pipes, namely high-density polyethylene (HDPE) pipes have been widely used in WDNs. The mechanical properties of HDPE pipes

(fracture mechanics properties, elastic modulus, and tensile strength) induce a different behaviour in the presence of a crack. Indeed, elastic pipeline with a sharp crack can be damaged even under a small load. Whereas, the viscoelastic properties of HDPE can present a different behaviour [2]. Under these circumstances, Linear Elastic Fracture Mechanics (LEFM) based on the Stress Intensity Factor K [3,4] cannot be applied since the strain at the crack tip is plastic.

To address this problem, a new branch of fracture mechanics has appeared in the period between sixties and the eighties of the last century. Consequently, the plastic behaviour of materials and the nonlinear or elasto-plastic fracture mechanics have been considered.

Even though a variety of methods are available to determine the properties of fracture mechanics for elasto-plastic materials, the procedure is still not standardized. As a result, the establishment of a consistent characterization procedure has been extremely delayed. Rice [5] and Bui [6] have introduced the energetic contour path integral (also referred to as J) to compute the release rate of the strain energy. The J -integral method have been widely used by engineers and researchers [7–9]. The procedure consists in plotting J - R curves based on standard compact tension tests (CT) to determine the fracture toughness of the material. Indeed, fracture toughness is considered highly significant in the characterization of a material its ability to resist to the crack propagation. Throughout the years, studies have demonstrated that the critical fracture toughness (J_{Ic}) of HDPE displayed significant variations, ranging from as low as 7 kJ/m² to above 20 kJ/m² [10]. More precisely, the values of J_{Ic} varies from one researcher to another, which makes it difficult to choose the convenient value.

A different criterion, in case of highly ductile materials, can be used when the plasticization at the end of the crack becomes significant. Crack Tip Opening Displacement (CTOD) criterion uses the crack tip gap to prevent cracking [11]. The crack tip opening displacement is measured with a Digital Image Correlation (DIC) camera and commercial digital image analysis software with distance- and angle-measuring tools.

In the present study, we aim to determine an exact value of the critical J -integral using both approaches. Firstly, the constitutive law of HDPE material based on tension tests will be determined. To this end, the material characteristics are first determined. The tests were carried out on a series of molded specimens and, subsequently, on a second extruded series. In a second part, the extension of a crack by means of tests conducted on specimens of compact tension (CT) is investigated. The test specimens were taken from an HDPE plate in three different directions to highlight an eventual anisotropy of our material. In a final stage, this criterion will be combined with the Crack-Tip-Opening-Displacement to find the value

of the critical J-integral.

2. Mechanical Properties of High-Density Polyethylene

In this section, the mechanical properties of HDPE material, namely the modulus of elasticity, elastic limit, elongation, proportional limit, reduction in area, tensile strength, yield point, and yield strength, are determined. This task is achieved by performing tensile tests on standard test specimens. The test specimen presented in Fig. 1 was manufactured according to the ISO 6259 procedure [12]. The various dimensions presented on the same figure are displayed in Table 1. It is to note that the values of the thickness and the width are 8 and 10 mm, respectively.

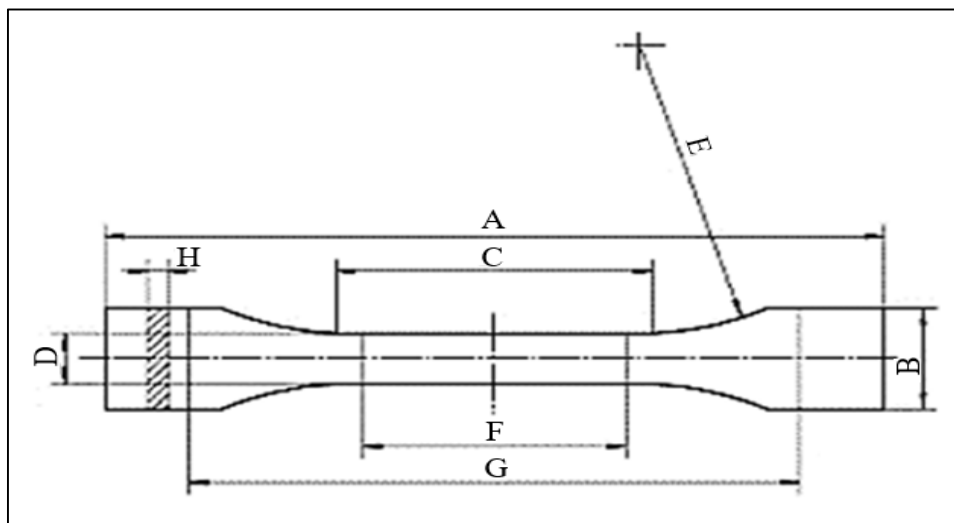


Fig. 1: Geometry of the test specimen

Table 1. Dimensions of the test specimens

Symbol	Discription	Dimensions (mm)
A	Overall length	150
B	Width of ends	20±0.2
C	Length of narrow, parallel-sided portion	60±0.5
D	Width of narrow, parallel-sided portion	10±0.2
E	Radius	60±0.5
F	Gauge length	50±0.5
G	Initial distance between grips	115±1.0
H	Thickness	8±0.2

2.1. Effect of strain rate

To determine the mechanical characteristics of HDPE material (CH₂-CH₂), the tension tests were performed at room temperature. Samples were extracted from the elbow according to the instructions of ISO 6259 [12] standard. The test specimens were cut from the molded 90 Degree elbow (**Fig. 2**). The dimensions of the elbow made of HDPE material are presented in

Table 2. The tension specimens were machined in two steps: cutting with a water jet to obtain the shape of the specimen was performed as a first step followed by surfacing operation by milling to reach the desired thickness. To account for the dispersion of the results, three tension tests were performed for each strain rate. In what follows, an average curve of the three measurements will be represented.

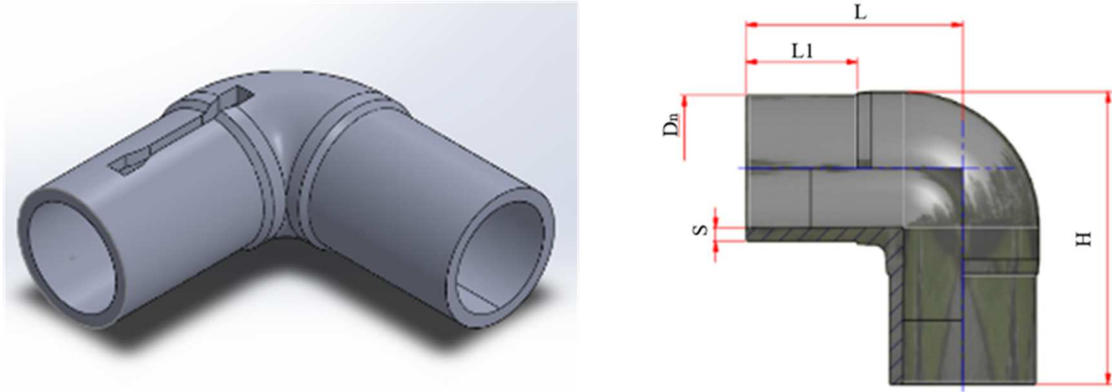


Fig. 2: Sampling of test specimens from the elbow

Table 2. Dimensions of the elbow

Dimension	Value (mm)
D _n	125
L1	95
L	184
S	11.4
H	250.5

The tension specimens are placed between two jaws of the machine and then stretched until they break. In the current case study, the elongation increases uniformly. Deformation of the specimen is measured during the test by a high-resolution universal tensometer, "MakroXtens II", which is displayed in Fig. 3. The machine used for these different tests, ZWICK Z250, is a universal machine. Its test strain rate varies between 0.0005 and 3000 mm/min. This machine is designed for loads up to 250kN. Furthermore, it can be piloted in force or in displacement. During the experiments, the parameters of the machine were modified according to a control software. For the current investigation, three different strain rates 10^{-3} , $5 \cdot 10^{-3}$, and 10^{-2} s^{-1} were chosen.

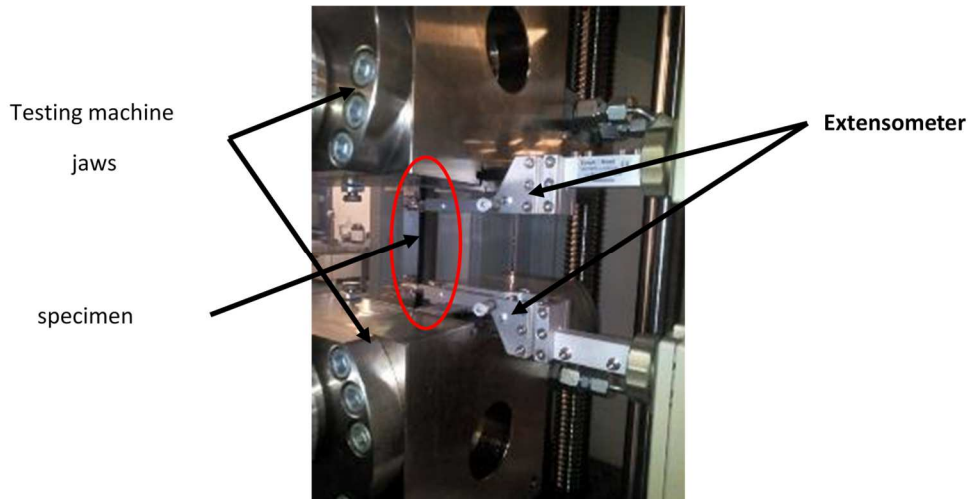


Fig. 3: Extensometer

Fig. 4 illustrates the measured engineering tension stress–strain curves for molded HDPE specimens at different crosshead strain rates. The mechanical characteristics, obtained from the three tension tests on specimens which were machined from a molded elbow, are summarized in Table 3. We note that the strain rate loading influences the behaviour of the material in two aspects. First, the elastic limit increases with the strain rate since the rigidity of the material will increase. The second aspect is the decrease in the elongation at break with increasing solicitation strain rate. It is to note that the obtained behaviour is related to the viscous component of the polyolefin material.

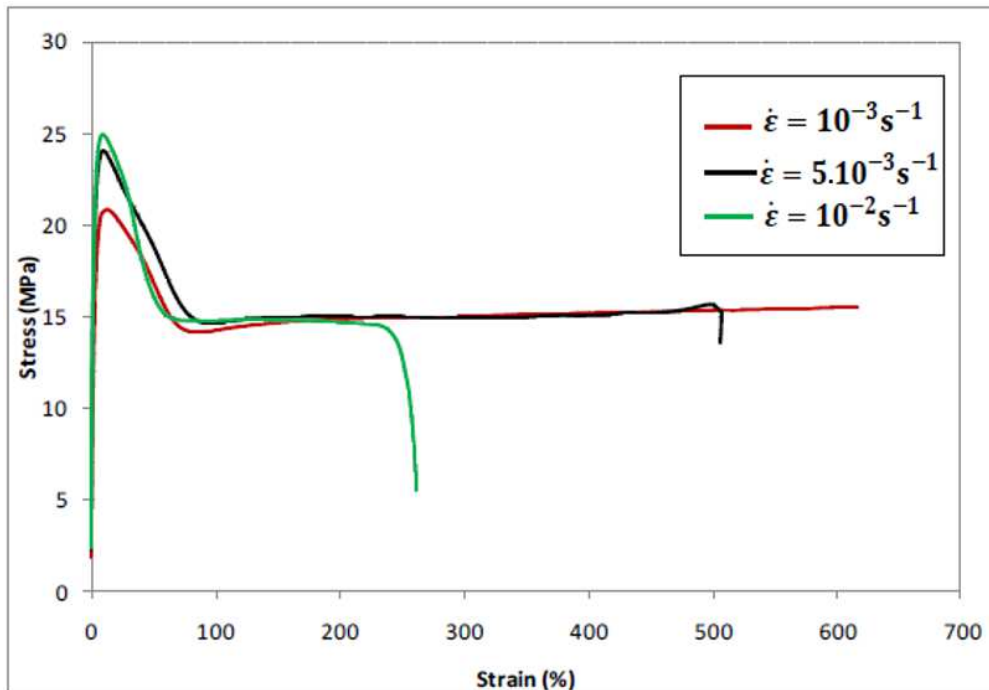


Fig. 4: Stress-strain curves for specimens machined from a molded HDPE elbow

Table 3. Mechanical characteristics of specimens machined from a molded HDPE elbow for three strain rates

Strain rates (s^{-1})	Young's modulus E (MPa)	Yield stress σ_y (MPa)	Ultimate strength σ_u (MPa)	Ultimate strain (%)
10^{-2}	1520.2	23.5	25.85	9.44
$5 \cdot 10^{-3}$	1458.6	22	24.92	9.06
10^{-3}	1346.4	17.5	22.08	10.12

Three different strain rates were first considered to investigate the effect of the strain rate on the mechanical characteristics of the material. Obtained experimental results are displayed in Table.3. It is clearly observed that a slight difference was obtained for the different values of strain rate. Therefore, only one value of the strain rate is considered for the following tests.

Experiments to study the impact of the specimen direction on the mechanical characteristics were conducted for a strain rate of 10^{-3} .

2.2. Influence of orientation

To perform a complete study of the behaviour and anisotropy of the HDPE material, it is necessary to use specimens in different directions ($\alpha = 0^\circ$, 45° and 90°) with respect to the extrusion direction of plates, as shown in the Fig. 5. Since the elbows are molded, HDPE plates were used to prepare the test specimens shown in Fig. 5. The results of uniaxial solicitation are presented according to the direction of sampling in the plane of the plate.

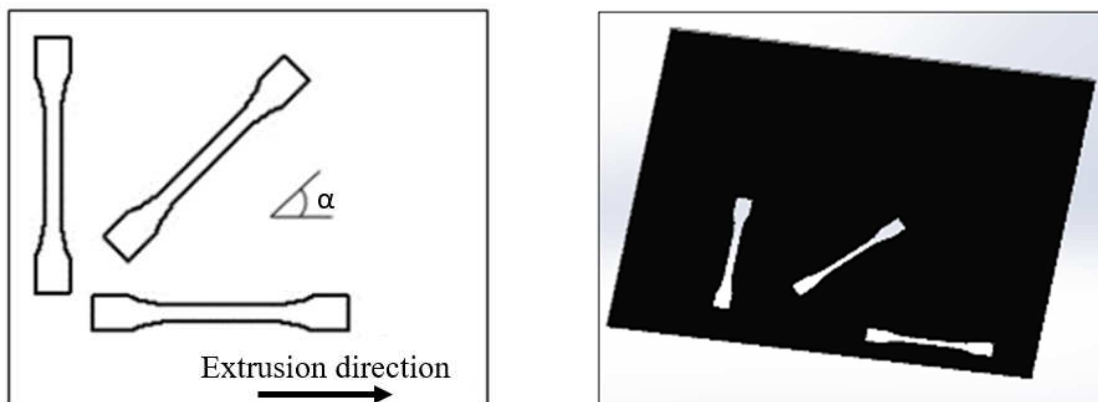


Fig. 5: Specimens cut from the extruded sheets in different directions

Fig. 6 depicts the stress-strain curves for the different orientations, obtained for a strain rate equal to $10^{-3} s^{-1}$. It is observed that the curves follow a relatively similar pattern up to a deformation equal to 200%. As a result, one can conclude that the PE100 material has a particularly isotropic behaviour. A further observation of Fig. 6 indicates that specimen's

deformation of the 0° and 45° orientation reached 210% and 240%, respectively. On the other hand, the deformation reached up to 370% for an orientation of 90°.

For a strain rate of 10^{-3} s^{-1} , a comparison was made between the tension tests results for specimens machined for different angles with respect to the extrusion direction (Fig. 6) and those machined from a molded elbow (Fig. 3). The obtained gap was found to be not exceeding 3%. Henceforth, it can be concluded that the high-density polyethylene PE100 is an isotropic material.

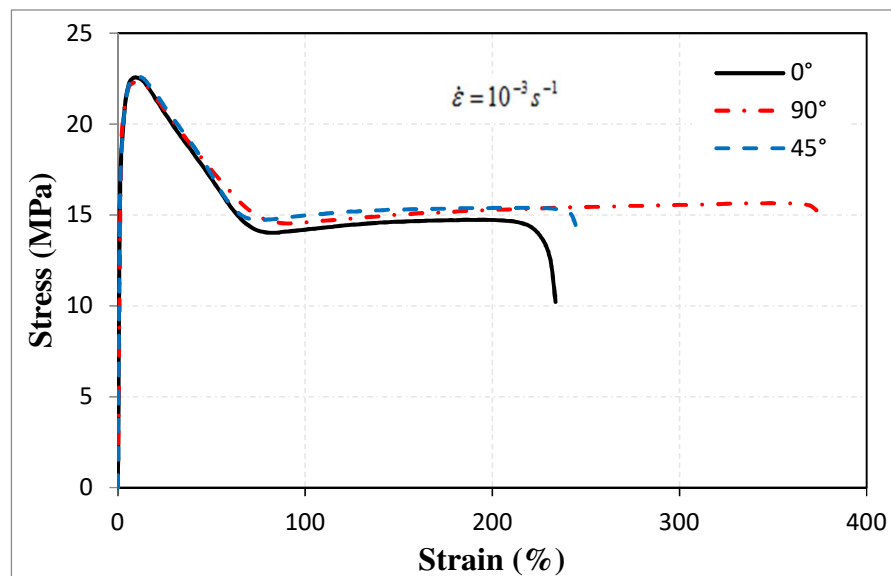


Fig. 6: Stress-strain curves for different angles

3. The J-integral

3.1. Objective

In this section, the initiation of defects in the structures is analysed based on the level of ductility of the material according to different concepts. For high density polyethylene, the strain at the crack tip is plastic. As a result, the approach of Linear Elastic Fracture Mechanics (LEFM) based on the Stress Intensity Factor K , is not applicable. Nevertheless, since the HDPE has a visco-elastoplastic behaviour, a second concept has been developed, i.e. non-linear fracture mechanics, which takes into consideration this type of material and all ductile materials in general. The toughness of HDPE material is represented by the curve of the J-integral ($J = f(\Delta a)$), corresponding to the rate of energy relaxation for the propagation of plane cracks. When the J-integral reaches the critical value (J_{Ic}), the crack propagates. J_{Ic} can be considered as a material parameter.

3.2. Specimen preparation

The compact tension (CT) specimen was standardized by the ISO 13586 standard [13]. Since the machining of specimens from a bent pipe is quite difficult, we have chosen to use 8 mm thick PE100 plates instead. For the rest of this study, all CT specimens were cut from a plate.

The dimensions of the specimens were determined in accordance with ASTM E1820. To establish a comprehensive study on this material, we machined specimens from extruded plates in three different directions ($\alpha = 0^\circ$, $\alpha = 45^\circ$ and $\alpha = 90^\circ$). Fig. 7 indicates that the directions are chosen with respect to the extrusion direction. Moreover, all results are presented according to the sampling direction. The initiation of the crack depends on the radius of the root pertaining to the initial pre-notch. A smaller pre-notch is more comparable to the geometry of a crack during propagation [14]. Therefore, a very fine pre-crack of 4 mm depth has been introduced at the bottom of the notch using a cutter blade.

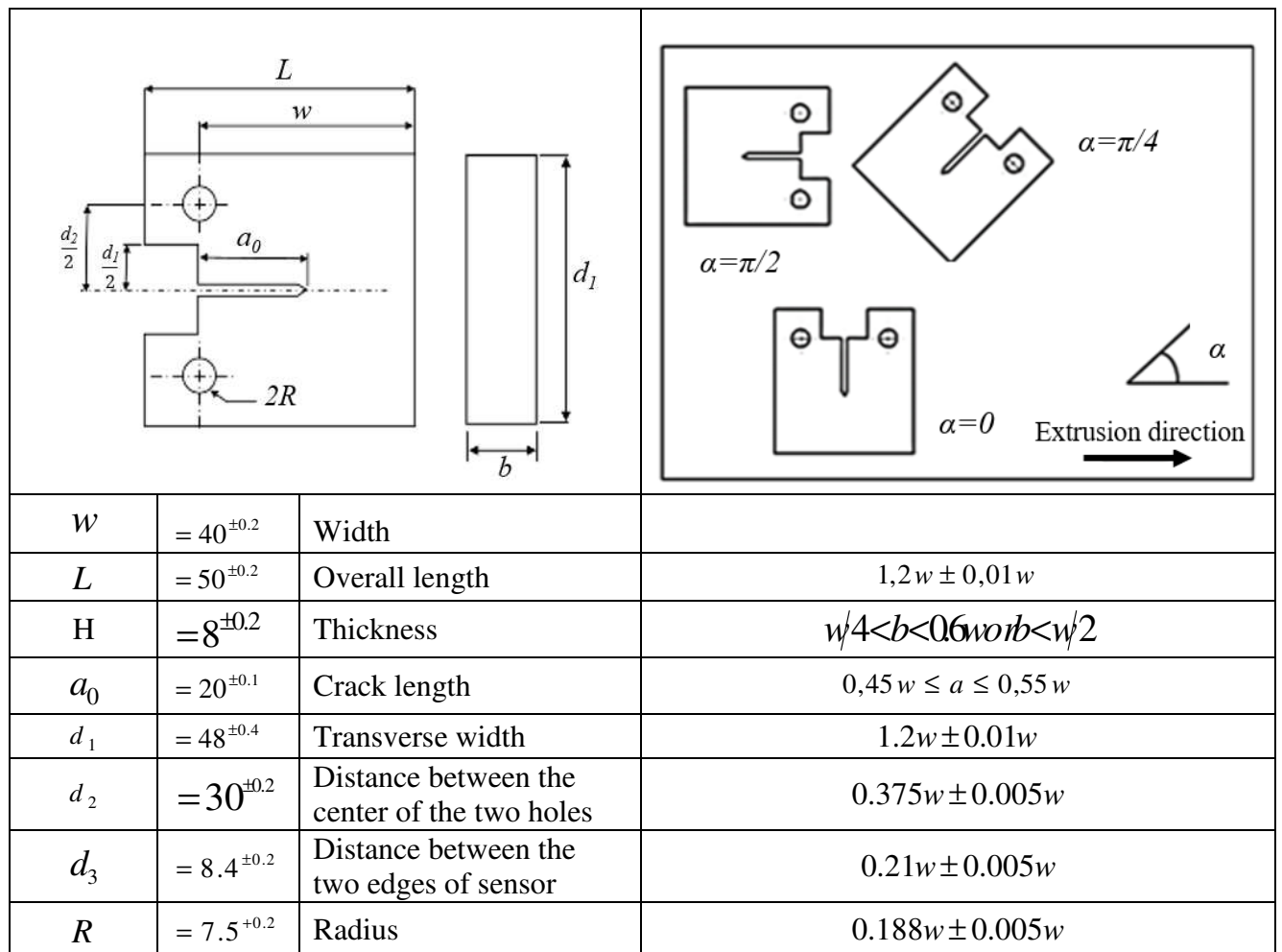


Fig. 7 : Standard compact tension (CT) (mm)

4. Experimental procedure of J-integral

In this section the experimental procedure for calculating the J-integral is introduced. Tension tests on CT specimens were performed by imposing a transverse displacement energy with a set speed of 0.05 mm/min and an ambient temperature of 20°. Tests were carried out on an INSTRON tension / compression machine. The mounting on the machine and the progress of the test are recommended by ASTM D6068.

For each sampling angle, the tests were carried out on seven test pieces with different levels of arrow or opening. Each specimen leads to the determination of the curve (load / displacement). Consequently, a coupling ($J, \Delta a$) in the J-R curve is obtained.

4.1. Method of determining the J-integral

Numerous methods were proposed in the literature to experimentally determine the J parameter. The researches of Sumpter and Rice et al. [15,16] have shown that the parameter J can be represented by Eq. (1).

$$J = \eta \frac{U}{H(W - a_0)} \quad (1)$$

In which, the term of energy U represents the difference between the total energy U_T and the indentation energy U_i . U_i was computed following a tension test, which is performed on an unnotched CT specimen (Fig. 8 (b)). The maximum load for this test was 10% higher compared to that obtained in testing notched CT specimens.

The η factor from Eq. (1) can be computed using the following equation (Eq. (2)) [17]:

$$\eta = 2 + 0.522 \left(1 - \frac{a}{W} \right) \quad (2)$$

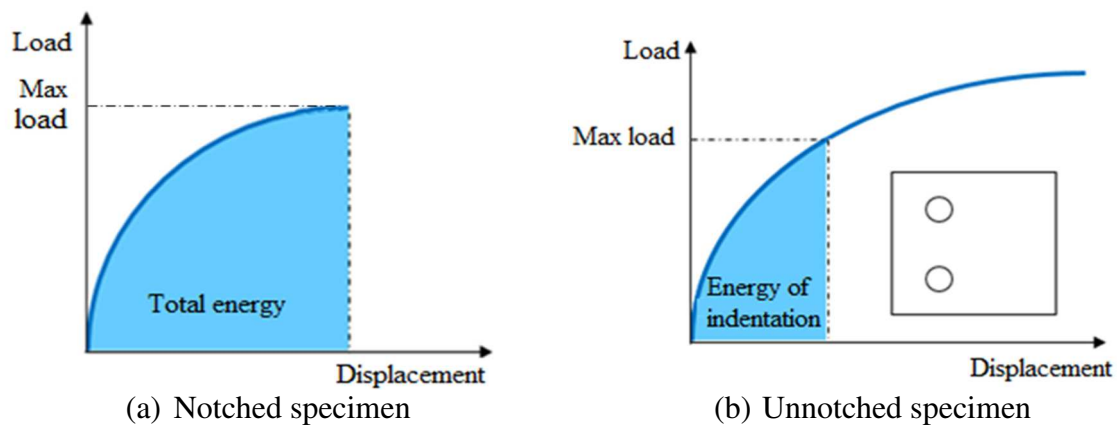


Fig. 8: Determination of total and indentation energy

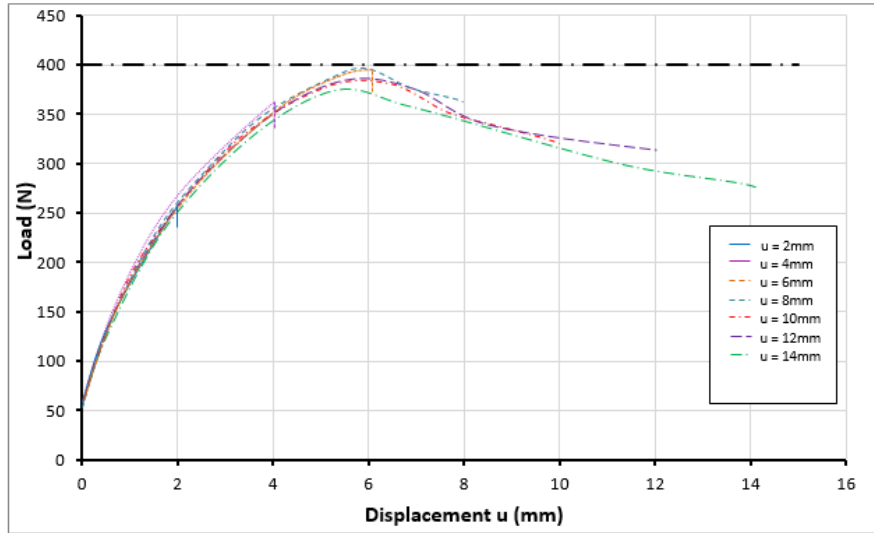


Fig. 9: Experimental load-displacement curves (Specimens 0°)

Fig. 9 presents the resulting load-displacement curves of the CT tests. The total energy U_T is therefore computed as the area under the load-displacement curve. It was found that the value of the maximum load is reached for a displacement in the vicinity of 6 mm, which corresponds to a load drop and a visible propagation of crack.

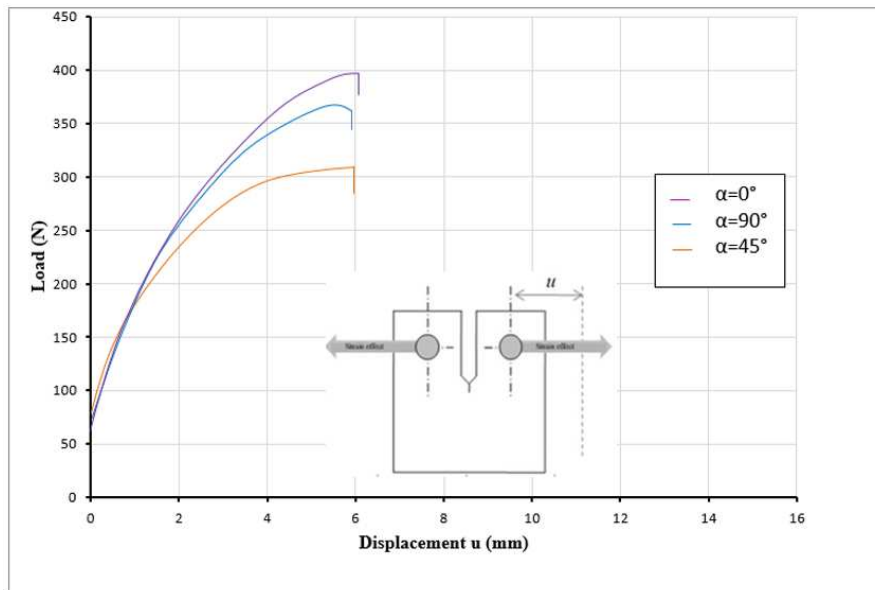


Fig. 10: Load-displacement curves for an imposed displacement of 6 mm

Considering an imposed displacement of 6 mm, the load-displacement curves for the three different angles are superposed in Fig. 10. A first glance indicates that each angle direction exhibits a different behaviour. The obtained dissimilarities can be elucidated by the orientation of the macro-molecular chains (micro-fibrils). As shown in Fig. 11, the propagation of the crack would be easier in the longitudinal direction since it is aligned with

micro-fibrils. However, it is not the same case for the transversal direction where the micro-fibrils are perpendicular to the crack direction. The obtained conclusion may also serve as an explanation for the variant behaviour of the specimens in Fig. 6. Fig. 12 presents a zoom of Fig. 6 for a strain larger than 200%. The difference of elongation for different angles of orientation can thus be attributed to the orientation of the micro-fibrils.

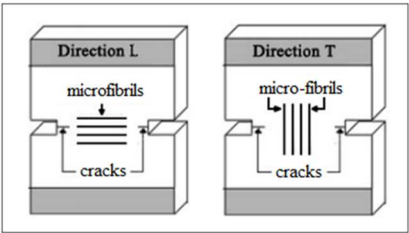


Fig. 11: Direction of micro-fibrils corresponding to the direction of sollicitation

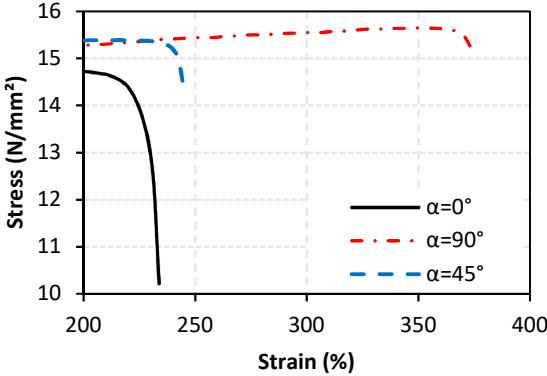


Fig. 12: Stress-strain curves for different angles

4.2. Crack-extension Δa

To represent the J-R curve, a coupling between J and the crack extension value (Δa) is required. To distinguish Δa from the other zones, the following steps are performed; First, a pre-crack zone P is created, followed by the CT test. As soon as the CT test is finished, a yellow paint is sprayed on the crack. The yellow paint serves as a marker of the two facies of the crack propagation, which will be considered for the microscopic observation and hence the determination of Δa. After perfect drying of the paint, the tension test was carried on at a higher strain rate of the order of 10³ s⁻¹ to break the specimen.

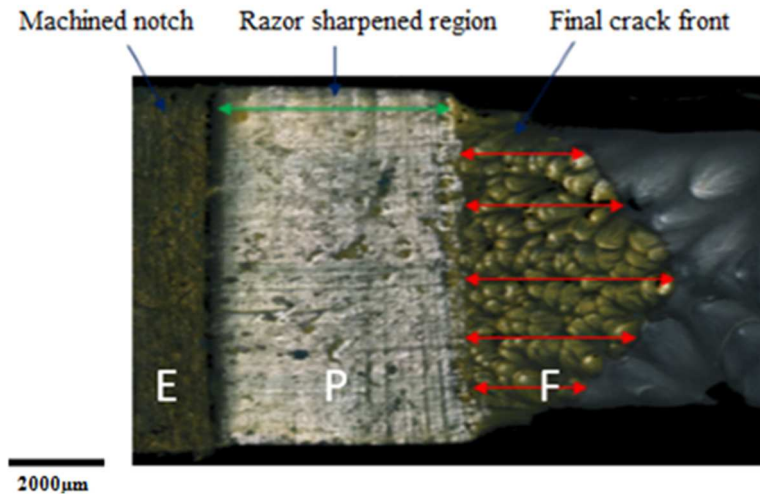


Fig. 13: Crack-extension measurements (Δa)

Fig. 13 depicts an observation, obtained by means of a 3D optical microscope "ALICONA", of the notch zone (E), the pre-crack zone (P) created by a cutter, and the crack propagation surface (F). Based on this observation, Δa is defined as the distance, marked in red arrows, between the front of the pre-crack and the front of the final crack. The final value of the crack extension is calculated as the average of five values measured at the five equidistant points marked in red.

The previous instructions were performed for the specimens obtained at different angles with respect to the direction of extrusion. The experiments were performed under various imposed displacement (2mm-14mm). Results of the calculated crack extension for the different cases are regrouped in Table 4.

Table 4. Crack extension values obtained for different specimen orientation

Imposed displacement u (mm)	2	4	6	8	10	12	14
Specimens 0°	0.3	0.37	1.5	3.06	4.17	4.865	7.1
Specimens 45°	0.5	0.626	1.15	2.47	4.42	5.04	5.7
Specimens 90°	0.3	0.4	1.6	2.4	3.79	5.82	6.1

Fig.14 displays the fracture facies on a scale that represents the crosshead displacement. As illustrated in the microscopic observations, the shape of the crack varies as a function of the imposed displacement. Precisely, the crack tip takes a parabolic shape, highlighted in red, as it propagates through the specimen.

At a given crosshead displacement between 6 and 8 mm, named d_{max} , the crack is already initiated over the entire thickness of the specimen. The denomination d_{max} comes from the fact that the maximum load, during the tension test CT, is obtained in the vicinity of this displacement where the crack tip takes a parabolic shape. After reaching d_{max} , the spread becomes faster and more stable, which results in a gradual decrease in applied loading as depicted in Fig. 9.

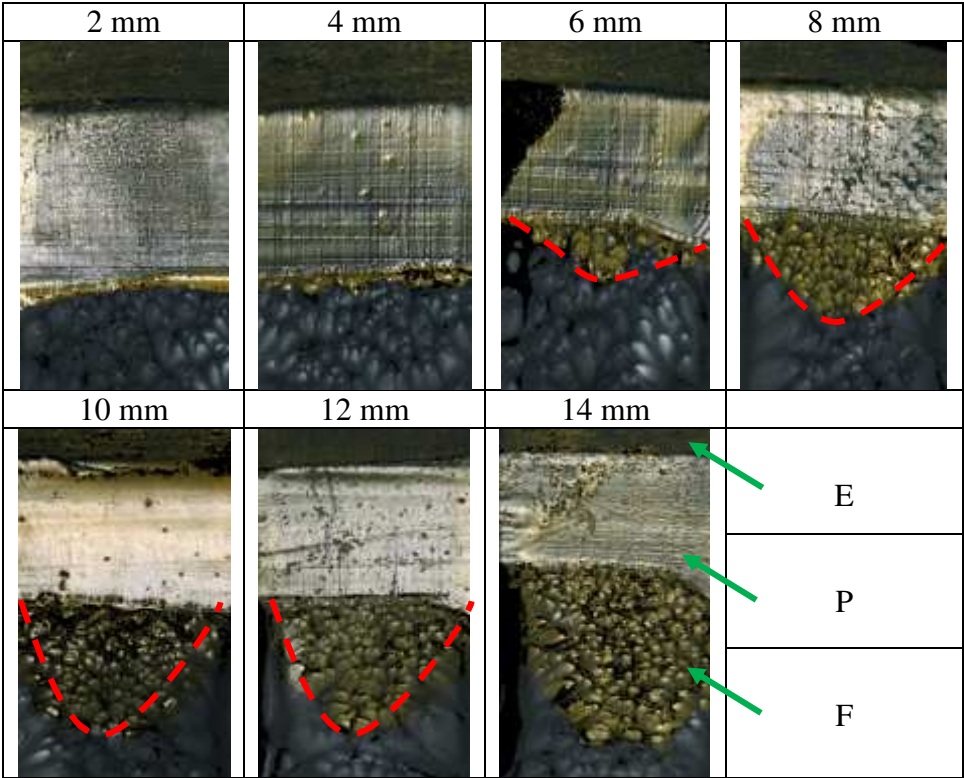


Fig. 14 : Crack-extension (Specimens 0°)

5. J-R curve and fracture toughness

As discussed previously, the total and indentation energies are required to calculate the J-integral. To this end, values of U_T and U_i are computed for the different cases described previously. To recall, the values of the energies are determined from the Load vs Displacement curve, as shown in Fig. 8.

For a better visualization of data, the CT test results are displayed in Table 5. The J-integral value is calculated through Eqs. (1) and (2). Obtained values are later used to plot the J-R curves. For the sake of simplicity, only the J-R curve of the Specimens 0° is presented, (see Fig. 15).

Table 5. Summary of the tests

Imposed displacement u (mm)	2	4	6	8	10	12	14
Specimens 0°							
Max-load (N)	250	360	382	395	370	378	365
Δa (mm)	0.3	0.37	1.5	3.06	4.17	4.865	7.1
Total energy U_T (10^{-3} J)	356.94	1065.08	1884.7	2494.64	3037.68	3423.56	3855.8
Indentation energy U_i (10^{-3} J)	38.1	48.5	50.5	52.1	49.5	50	49
$U_T - U_i$ (10^{-3} J)	318.84	1016.58	1834.2	2442.54	2988.18	3373.59	3806.8
J (kJ/m ²)	1.99	6.35	11.46	15.26	18.67	21.08	23.79
Specimens 45°							
Max-load (N)	210	275	280	285	294.5	297.8	292
Δa (mm)	0.5	0.626	1.15	2.47	4.42	5.04	5.7
Total energy U_T (10^{-3} J)	332.16	972.68	1348.9	2027.966	2427.64	2977.9	3386.03
Indentation energy U_i (10^{-3} J)	33.8	40.2	41	41.5	42.2	43	42
$U_T - U_i$ (10^{-3} J)	298.35	932.48	1307.9	1986.47	2385.44	2934.9	3344.03
J (kJ/m ²)	1.86	5.28	8.17	12.41	15.02	18.34	20.9
Specimens 90°							
Max-load (N)	255	341	363	364	370	366	370
Δa (mm)	0.3	0.4	1.6	2.4	3.79	5.82	6.1
Total energy U_T (10^{-3} J)	353.87	973.427	1837.257	2399.42	3189.61	3892.53	4457.02
Indentation energy U_i (10^{-3} J)	38.4	46.5	48.5	48.7	49.5	49	49.5
$U_T - U_i$ (10^{-3} J)	315.47	926.927	1788.5	2350.72	3140.11	3843.53	4407.52
J (kJ/m ²)	1.97	5.79	9.17	14.69	19.62	22.77	27.54

The interpolation proposed by Hiser and Loss [18] is used to determine the equation of J-integral variation as a function of the crack extension. Specifically, they have proposed the use of smoothing points by means of a power function that exhibit the following form:

$$J = c_1 \Delta a^{c_2} \quad (3)$$

In which c_1 and c_2 are constants, and Δa is the crack extension.

$$Y = 7.44x^{0.650} \quad (4)$$

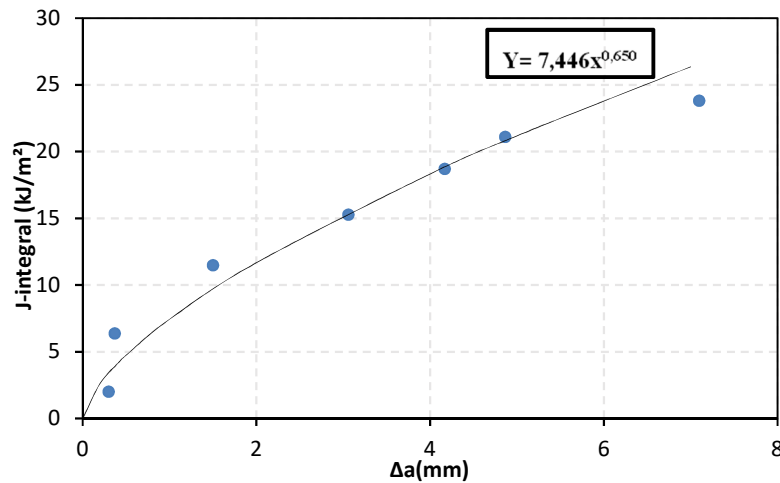


Fig. 15: J - Δa diagram of HDPE, including blunting line (Specimens 0°)

5.1. First method to determine the of J_{Ic}

When applying a load on specimens, a blunting in the crack tip is generated. The J values, hence, follows the following law [19]:

$$J = \beta \cdot \Delta a \quad (5)$$

Where β is a constant that depends on the tensile characteristics of the material.

According to Beaver et al.[20] the value of the constant β can be expressed as follows:

$$\beta = 2\sigma_y \quad (6)$$

In which σ_y represents the average of the yield strength R_e and the maximum stress R_m .

The standard ASTM E 813 [21] indicates that the toughness J_{Ic} should be calculated as the intersection of the J-R curve and the blunting curve shifted by 0.2 mm. Henceforth, the following equation will be considered to express the J values:

$$J = 2\sigma_y \cdot (\Delta a - 0.2) \quad (7)$$

Based on these instructions, the fracture toughness is described as the intersection of the blunting line with the J-R curve as illustrated in Fig. 16. Using this method, the value of fracture toughness was calculated for each angle. Despite the isotropy of the studied material, the obtained values of J_{Ic} (between 1.9 and 3.2kJ/m²) are different compared to those presented in the literature (between 7 and 20 kJ/m²) [22]. Consequently, this method is considered not reliable to determine the toughness of HDPE.

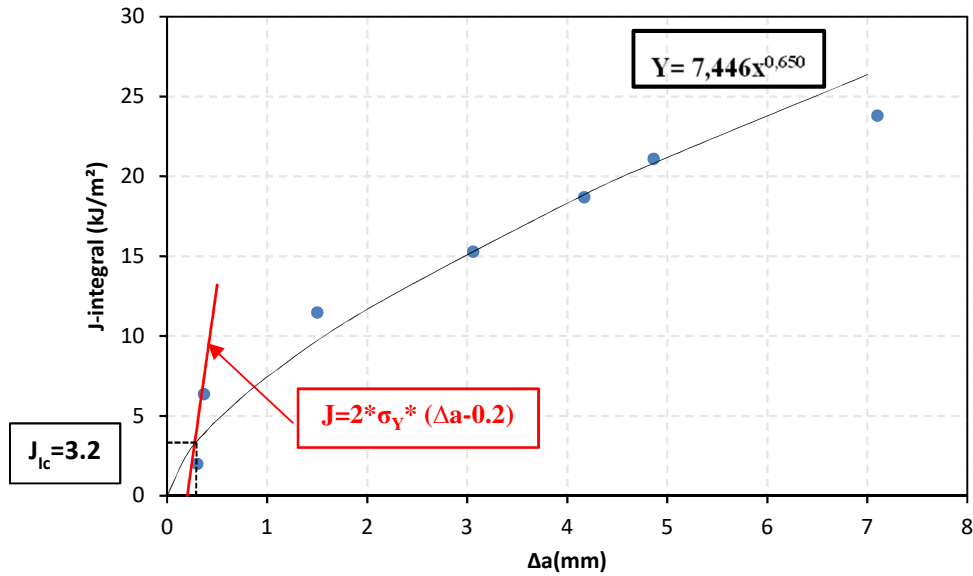


Fig. 16: J - Δa diagram of HDPE, including blunting line (Specimens 0°)

5.2. The Second method to determine the value of J_{1c}

A second method to determine the critical value of the J-integral from the J-R curve has been studied by various authors; namely Pluvinage [23], Dzugan et al.[24], and Kim et al. [25]. In the case of a ductile material, this method indicates that the experimental J-R curve follows two linear functions. The first function characterizes the blunting of the crack during loading and it is expressed as follows:

$$J = \beta \cdot \Delta a \tag{8}$$

The second linear function represents the stable growth of the crack. The intersection between these two functions represents the crack propagation moment (fracture toughness). The usage of this method is illustrated in Fig. 17.

Using this second method, we observed J_{1c} values (between 5.02 and 7.38kJ/m²) in accordance with the values found by Bouaziz (equals to 7.69kJ/m²) [26].

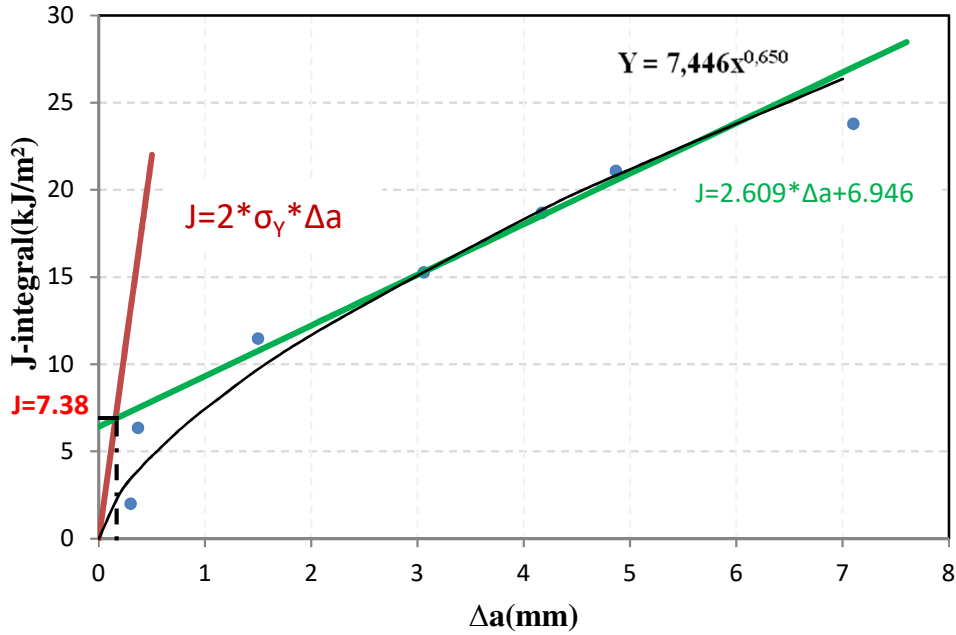


Fig. 17: J-R curve of HDPE (Specimens 0°)

A comparison between the results of the tension tests on the two series of CT specimens using the two methods are compared in Table 6. It is obvious that fracture toughness values obtained using the second method are approximately twice larger than those obtained using the first method.

Table 6. Resistance to cracking of PE100 (kJ/m²)

Angle	0°	90°	45°
First method	3.2	2.72	1.9
Second method	7.38	5.87	5.02

The precision of the J-R curve highly depends on the material, the geometry of the specimens, the loading method, and the precision of the different measurements taken along the procedure. Due to these uncertainties of the critical value of the integral J, a study of a failure criteria with the Crack Tip Opening Displacement CTOD is proposed in the following section.

Following the standards ASTM E1820 [27] and ASTM D6068 [28] the curves describing the energy conditions, required for an additional propagation of the crack initiation, can be established as well as that of CTOD according to the advance of the crack. Specifically, these curves describe the case of a slow crack propagation, stable in mode I and in a state of plane deformations in an elastoplastic material.

6. Crack-Tip- Opening-Displacement-CTOD measurement

6.1. Test procedure

In fracture mechanics, the resistance to cracking is described by expressing the crack tip opening displacement (CTOD) as a function of crack propagation Δa . Tests on CT specimens were performed using different orientation angles (0° , 45° and 90°). After pre-cracking, the specimens were painted white to enhance contrast with the black background. Using the same Instron 1341 hydraulic tension/compression machine, the sample was attached to both jaws via two pins. The loading of the tension test was controlled using the INSTRON Wavemaker software, which records the movement of the cylinder and the applied force (DIAdem software). An Olympus camera (500i /s), with two lighting flashes, was used for image acquisition (Fig. 18). The camera is used to record the crack initiation on specimens.



Fig. 18: Experimental test set-up

6.2. Results

Fig. 19 illustrates how the CTOD can be measured [30]. Accordingly, the recordings were performed during the loading measure of CTOD as a function of the depth of the 'Stretched Zone Width' SZW blunting zone. According to the American standard ASTM (E 2472) [29], the mean value of the SZW zone is between 0.5 and 1.5 mm. To obtain satisfactory results, 30 different images at different instants were selected. In other terms, these recordings will be used to determine the values of CTOD as it propagates with time.

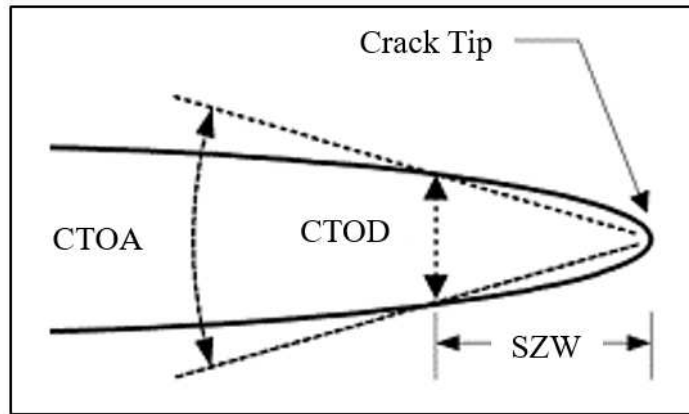


Fig. 19: Definition of CTOD and CTOA [30]

Once a test was completed, the entire video-taped history was reviewed to measure CTOD and the crack extension. Fig. 20 indicates the location where CTOD was measured. Using length measurement tools, the crack extension was measured from the crack tip location from the previously selected image and the final crack tip location and recorded for each stable tearing event [29].

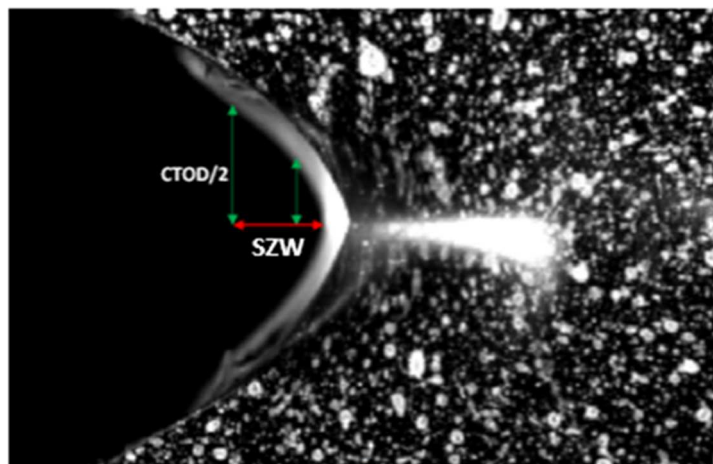


Fig. 20: Example of CTOD and crack-extension measurements

To obtain the value of the critical J- integral, all results obtained for test specimens with different orientation angles were used. In other terms, the data are plotted in the same figure. The results displayed in Fig. 21 represents the variation of the CTOD as a function of the crack advance Δa . The crack starts to propagate when the CTOD reaches a critical value. The method used to determine the critical CTOD is according to the ASTM E1820 recommendation.

The CTOD curve as a function of Δa exhibit a relatively rapid increase. Therefore, the blunting equation can be expressed by the following equation (norm: ASTM E1820):

$$CTOD = 1.4\Delta a \tag{9}$$

However, it is difficult to experimentally determine the ductile initiation instant. Therefore, the standards indicate that the crack initiation is defined from the propagation value $\Delta a=0.2$ mm. The blunting line is thus shifted by 0.2 mm on the abscissa as indicated in Fig. 21.

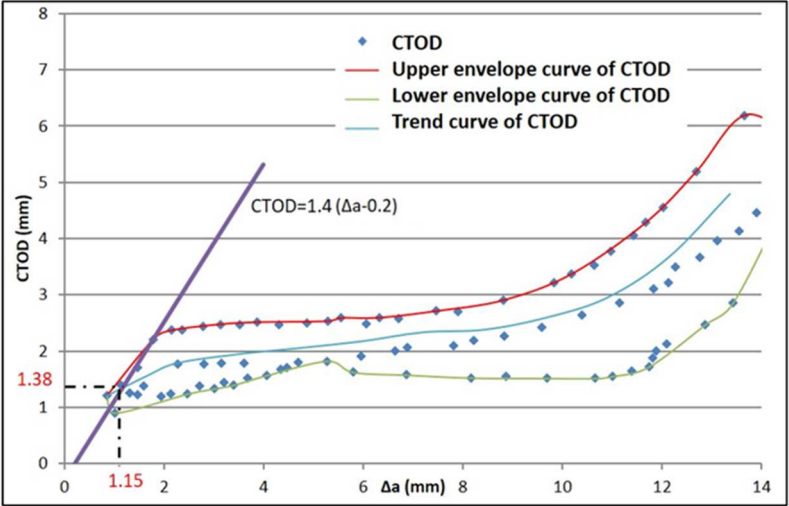


Fig. 21: CTOD R-curves

Normally, the critical value of the CTOD is computed from the intersection of the blunting line with the CTOD curve. However, a further observation from Fig. 21 reveals that data points are almost overlapping at the beginning of the CTOD test. Consequently, Data envelopment technique was used to determine the trend curve of CTOD. Using the obtained trend curve in Fig. 20, the $CTOD_c$ value for tension CT specimens was found equal to 1.38 mm. This value corresponds to a crack extension equal to 1.15 mm.

6.3. Discussion

To obtain one critical value of J-integral, data envelopment analysis was used for CT test results for all specimens. Fig. 22 displays the upper envelope curve, the lower envelope curve, and the mean curve of CT tests results. By placing the value of the critical crack advance, determined from the crack opening curve in the average crack resistance curve (Fig. 21), we show that the value of the critical J-integral is equal to 8.4 kJ/m². The value of the J-integral is determined by referring to the J-R curves (Fig. 15), and projecting the value of $\Delta a = 1.15$ mm on the curve J-R.

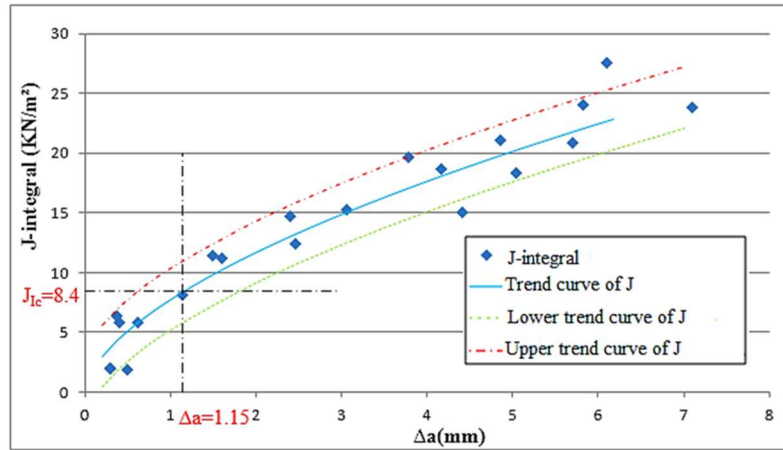


Fig. 22: Crack growth resistance curve (R-curve)

Table 7 indicates that the difference between the values obtained using the second method and those obtained using the CTOD method varies between 9.5% and 28% for the three considered angles. Meanwhile, the first method presents a difference in the calculated values up to 60%. It is worth noting that the new J_{Ic} values are closer to the values found using the second method. Consequently, one can conclude that the first method should not be considered for calculating the critical value of the J-integral.

Table 7. Resistance to cracking of PE100 (kJ/m²)

Angle	First method	Second method	For $\Delta a=1.15$ mm
0	3.2	7.38	8.15
90	2.72	5.87	8.16
45	1.9	5.02	6.2

7. Conclusions

In this paper, the critical value of the J-integral was determined experimentally for HDPE elbow. Basing on tension tests performed on specimens machined for different angles with respect to the extrusion direction, it was demonstrated that high-density polyethylene PE100 is an isotropic material. The curves of the J-integral as a function of the crack-extension were later plotted based on the tension tests performed on CT specimens. To calculate the critical value of the J-integral, two methods were used. It was shown that the results of these methods present large dissimilarities in the fracture toughness values. Correspondingly, a study of a failure criteria with the crack tip opening displacement (CTOD) was proposed. Basing on the combination of the ASTM D6068 with J-R curve and the ASTM E1820 with the crack tip opening displacement (CTOD), the initiation fracture toughness (J_{Ic}) was determined. The obtained value of 8.4 kJ /m² is considered quite logical because the fracture toughness for

HDPE determined using only the J-integral methods showed significant variations, ranging from as low as 7 kJ/m² to above 20 kJ/m² [10].

References

- [1] A. Maddocks, R.S. Young, P. Reig, Ranking the World's Most Water-Stressed Countries in 2040, (2015). <https://www.wri.org/blog/2015/08/ranking-world-s-most-water-stressed-countries-2040>.
- [2] L. Hadj Taieb, N. Bettaieb, M.A. Guidara, S. Elaoud, E. Haj Taieb, Effect of integrating polymeric pipes on the pressure evolution and failure assessment in cast iron branched networks, *Engineering Fracture Mechanics*. (2020) 107158.
- [3] A.P. Mouritz, *Introduction to Aerospace Materials*, Woodhead Publishing, 2012.
- [4] A.A. Griffith, VI. The phenomena of rupture and flow in solids, Royal Society. (1920). <https://doi.org/10.1098/rsta.1921.0006>.
- [5] J.R. Rice, A path independent integral and the approximate analysis of strain concentration by notches and cracks, *Journal of Applied Mechanics, Transactions ASME*. 35 (1964) 379–388. <https://doi.org/10.1115/1.3601206>.
- [6] H.D. Bui, Dual path independent integrals in the boundary-value problems of cracks, *Engineering Fracture Mechanics*. 6 (1974) 287–296. [https://doi.org/10.1016/0013-7944\(74\)90027-7](https://doi.org/10.1016/0013-7944(74)90027-7).
- [7] H. Okada, S. Kadowaki, M. Suzuki, Y. Yusa, J-integral computation for elastic-plastic materials with spatially varying mechanical properties, *Engineering Fracture Mechanics*. 207 (2019) 181–202. <https://doi.org/10.1016/j.engfracmech.2018.12.029>.
- [8] M. Metzger, T. Seifert, C. Schweizer, Does the cyclic J-integral ΔJ describe the crack-tip opening displacement in the presence of crack closure?, *Engineering Fracture Mechanics*. 134 (2015) 459–473. <https://doi.org/10.1016/j.engfracmech.2014.07.017>.
- [9] R.C. McClung, G.G. Chell, S. Antonio, Development of a Practical Methodology for Elastic-Plastic and Fully Plastic Fatigue Crack Growth, (n.d.) 538.
- [10] A.S. Saleemi, J.A. Nairn, The plane-strain essential work of fracture as a measure of the fracture toughness of ductile polymers, *Polym. Eng. Sci*. 30 (1990) 211–218. <https://doi.org/10.1002/pen.760300404>.
- [11] A.A. Wells, Unstable crack propagation in metals-cleavage and fast fracture, in: Cranfield, 1961: pp. 210–230.
- [12] ISO 6259-3, Thermoplastics pipes — Determination of tensile properties — Part 3: Polyolefin pipes, International Organization for Standardization. (2015).
- [13] ISO 13586, Plastics - Determination of fracture toughness (GIC and KIC) - linear elastic fracture mechanics (LEFM) approach, (2000).
- [14] D. Grégoire, H. Maigre, J. Réthoré, A. Combescure, Dynamic crack propagation under mixed-mode loading – Comparison between experiments and X-FEM simulations, *International Journal of Solids and Structures*. 44 (2007) 6517–6534. <https://doi.org/10.1016/j.ijsolstr.2007.02.044>.
- [15] J.D.G. Sumpter, Jc determination for shallow notch welded bend specimens, *Fat Frac Eng Mat Struct*. 10 (1987) 479–493. <https://doi.org/10.1111/j.1460-2695.1987.tb00498.x>.
- [16] J.R. Rice, P.C. Paris, J.G. Merkle, Some Further Results of J-Integral Analysis and Estimates, in: J. Kaufman, J. Swedlow, H. Corten, J. Srawley, R. Heyer, E. Wessel, G. Irwin (Eds.), *Progress in Flaw Growth and Fracture Toughness Testing*, ASTM International, West Conshohocken, PA, 1973: pp. 231–245. <https://doi.org/10.1520/STP49643S>.
- [17] G. Clarke, J. Landes, Evaluation of the J Integral for the Compact Specimen, *Journal of Testing and Evaluation*. 7 (1979) 264–269. <https://doi.org/10.1520/JTE10222J>.

- [18] A. Hiser, F. Loss, Alternative Displacement Procedures for J-R Curve Determination, Elastic-Plastic Fracture Test Methods: The User's Experience. (1985) 263–277. <https://doi.org/doi.org/10.1520/STP34529S>.
- [19] M. Elmegueni, M. Naït-Abdelaziz, F. Zaïri, J.M. Gloaguen, Fracture characterization of high-density polyethylene pipe materials using the J -integral and the essential work of fracture, *Int J Fract.* 183 (2013) 119–133. <https://doi.org/10.1007/s10704-013-9848-x>.
- [20] P.W. Beaver, M. Heller, T.V. Rose, Determination of JIC for 2024-T351 aluminium alloy, *Fat Frac Eng Mat Struct.* 10 (1987) 495–506. <https://doi.org/10.1111/j.1460-2695.1987.tb00499.x>.
- [21] ASTM E813-89, Standard test method for JIc, a measure of fracture toughness, (1990).
- [22] M.A. Guidara, M.A. Bouaziz, C. Schmitt, J. Capelle, E. Haj Taïeb, Z. Azari, S. Hariri, Structural integrity assessment of defected high density poly-ethylene pipe: Burst test and finite element analysis based on J-integral criterion, *Engineering Failure Analysis.* 57 (2015) 282–295. <https://doi.org/10.1016/j.engfailanal.2015.07.042>.
- [23] G. Pluvinage, Fatigue and fracture emanating from notch; the use of the notch stress intensity factor, *Nuclear Engineering and Design.* 185 (1998) 173–184. [https://doi.org/10.1016/S0029-5493\(98\)00183-6](https://doi.org/10.1016/S0029-5493(98)00183-6).
- [24] J. Dzugan, P. Konopik, M. Rund, Fracture Toughness Determination with the Use of Miniaturized Specimens, in: P.H. Darji, V.P. Darji (Eds.), *Contact and Fracture Mechanics*, InTech, 2018. <https://doi.org/10.5772/intechopen.73093>.
- [25] Y.S. Kim, Yu.G. Matvienko, H.C. Jeong, Development of Experimental Procedure Based on the Load Separation Method to Measure the Fracture Toughness of Zr-2.5Nb Tubes, *KEM.* 345–346 (2007) 449–452. <https://doi.org/10.4028/www.scientific.net/KEM.345-346.449>.
- [26] M.A. Bouaziz, M.A. Guidara, C. Schmitt, E. Hadj-Taïeb, Z. Azari, I. Dmytrakh, Structural integrity analysis of HDPE pipes for water supplying network, *Fatigue and Fracture of Engineering Materials and Structures.* 42 (2019) 792–804. <https://doi.org/10.1111/ffe.12951>.
- [27] A. E1820, Standard Test Method for Measurement of Fracture Toughness, American Society for Testing and Materials. (2003).
- [28] A.S. D6068, Standard Test Methods for Determining J–R Curves of Plastic Materials Annual Book of ASTM Standards, *Plastics General Test Method.* (2010).
- [29] ASTM E 2472-06, Annual Book of ASTM Standards, Vol. 03.01., American Society for Testing and Materials. (2007).
- [30] S. Mahmoud, K. Lease, The effect of specimen thickness on the experimental characterization of critical crack-tip-opening angle in 2024-T351 aluminum alloy, *Engineering Fracture Mechanics.* 70 (2003) 443–456. [https://doi.org/10.1016/S0013-7944\(02\)00130-3](https://doi.org/10.1016/S0013-7944(02)00130-3).
- [31] P.A. Wawrzynek, R. Ingraffea, Crack Growth Simulation and Residual Strength Prediction in Airplane Fuselages, (1999) 189.